Topography Simulation of 4H-SiC-Chemical-Vapor-Deposition Trench Filling Including an Orientation-Dependent Surface Free Energy

Kazuhiro Mochizuki
Advanced Power Electronics Research Center
National Institute of Advanced Industrial Science and Technology
Tsukuba, Japan
k-mochiduki@aist.go.jp

Shiyang Ji
Advanced Power Electronics Research Center
National Institute of Advanced Industrial Science and Technology
Tsukuba, Japan
aist-ki@aist.go.jp

Ryoji Kosugi
Advanced Power Electronics Research Center
National Institute of Advanced Industrial Science and Technology
Tsukuba, Japan
r-kosugi@aist.go.jp

Yoshiyuki Yonezawa
Advanced Power Electronics Research Center
National Institute of Advanced Industrial Science and Technology
Tsukuba, Japan
yoshiyuki-yonezawa@aist.go.jp

Hajime Okumura
Advanced Power Electronics Research Center
National Institute of Advanced Industrial Science and Technology
Tsukuba, Japan
h-okumura@aist.go.jp

***Abstract*—Topography simulation of chemical-vapor-deposition (CVD) trench filling has been advanced as a tool for designing fabrication processes of high-voltage 4H-SiC superjunction devices. In the longitudinal section of filled stripe trenches, an experimentally observed dip, which had not been well reproduced with a previous technique using a fixed surface free energy γ, came to be qualitatively reproduced by including an orientation dependence of γ.**

Keywords—SiC, CVD, trench, surface free energy, orientation

I. Introduction

A 4H-SiC superjunction (SJ) power device [1], in which alternating p- and n-type columns are located in a drift layer [2], is expected to have the lowest specific on-resistance among wide-bandgap unipolar devices with breakdown voltage BV exceeding about 4 kV [3]. Although ion implantation has been used to fabricate 0.8−1.5 kV SiC SJ devices [4−6], chemical-vapor-deposition (CVD) trench filling, whose growth window was empirically obtained [7], should become the key technique for higher-BV SJ devices. With respect to trench filling of Si, ballistic-transport models have been used [8−11] because of large Knudsen number in low pressure CVD [12, 13]. In the case of CVD trench filling flowing SiH_4+C_3H_8+HCl+H_2, on the other hand, subatmospheric pressure (0.1−0.7 atm [7, 14−16]) has been used because of much larger equilibrium vapor-phase concentration of Si at higher growth temperature [17]. Based on a continuum-diffusion model [18−20], the reported cross section of 3-μm-pitch stripe trenches [that were formed on a (0001) substrate (i.e., A-A' in Fig. 1) and were filled under the conditions listed in Table I] [7] has been numerically reproduced up to 2 h by including the Gibbs−Thomson effect on the most dominant Si-containing growing species (i.e., SiCl) under a C-rich atmosphere:

$$C_{\mathrm{SiCl}}^{\mathrm{e}}(r, T_{\mathrm{s}}) = C_{\mathrm{SiCl}}^{\mathrm{e}}(\infty, T_{\mathrm{s}}) \exp[\gamma V_{\mathrm{m}}/RT_{\mathrm{s}}r], \quad (1)$$

where $C_{\mathrm{SiCl}}^{\mathrm{e}}$ is the equilibrium vapor-phase concentration of SiCl molecules that are in contact with a surface (with a radius of curvature r) at temperature T_{s}, R is the ideal gas constant, V_{m} is the molar volume of 4H-SiC, and the surface free energy γ was used as a fitting parameter (i.e., 0.1 J/m^2) [3].

With respect to the longitudinal section (i.e., B-B' in Fig. 1), on the other hand, an experimentally observed dip [Fig. 2(b)] has yet to be well reproduced with Eq. (1) [Fig. 2(a)]. In the case of Si trench filling in low pressure CVD, such a dip is unlikely to appear because a filling layer uniformly grows on

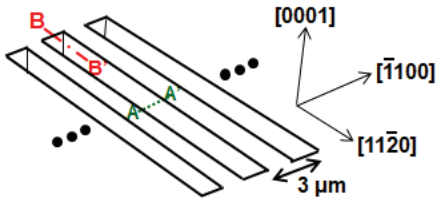

Fig. 1. Schematic perspective view of 3-μm-pitch SiC trenches formed along the [11-20] direction [3, 7].

This work was supported by Council for Science, Technology and Innovation (CSTI), Cross-ministerial Strategic Innovation Promotion Program (SIP), "Next-generation power electronics/Consistent R&D of next-generation SiC power electronics" (funding agency: NEDO).

TABLE I. CVD GROWTH CONDITIONS USED FOR TRENCH FILLING [3, 7]

SiH_4	7.5 sccm
C_3H_8	2.5 sccm
HCl	0.3 slm
H_2	80 slm
trimethylaluminum	1.28 μmol/min
pressure	0.38 atm
temperature	1873 K

both the bottom and sidewalls of trenches [21]. Numerical reproduction of a dip in the longitudinal section is therefore the specific challenge faced by CVD in the small-Knudsen-number regime.

4H-SiC has polar faces, i.e., (000-1) [Fig. 3(a)] and (0001) [Fig. 3(b)]; γ should thus depend on the crystallographic orientation [i.e., θ in Fig. 3(c)]. However, topography simulation of 4H-SiC CVD trench filling has never been carried out including a θ dependence of γ. Accordingly, in this study, θ-dependent γ was first included in the topography simulation to reproduce a dip in the longitudinal section.

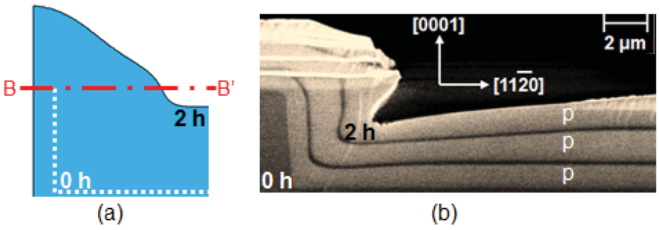

Fig. 2. Longitudinal sections (B-B' in Fig. 1) of SiC trenches (a) simulated with Eq. (1) using a constant γ of 0.1 J/m^2 and (b) observed using the same specimen reported in [3, 7]. The dark lines in (b) are intentionally grown n-type marker layers between each hour of growth.

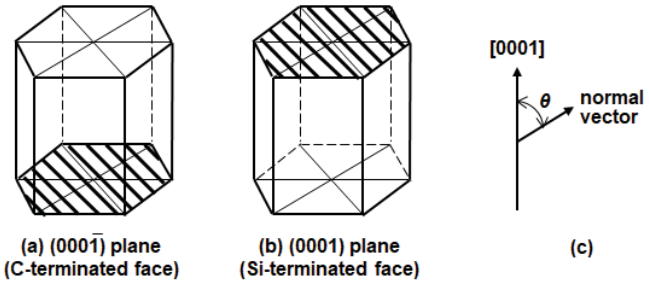

Fig. 3. (a) (b) Typical crystal planes and (c) definition of θ.

II. MODELING

A. Modeling of an orientation dependence of surface free energy

The dependence of γ on φ in spherical polar coordinates was neglected because of the similar crystal shapes observed for 4H-SiC grown at 1893 K on mesas along the [11-20] and [1-100] directions [22]. In the case $0^o \le \theta \le 90^o$, surfaces with θ of 0^o and 90^o only were reported to be singular (i.e., having no kinks where atoms are contained in a crystalline phase) [22]; $\gamma(\theta)$ is therefore expressed as [23]

$$\gamma(\theta) = \gamma(0^o)\cos\theta + \gamma(90^o)\sin\theta \quad (0^o \le \theta \le 90^o). \qquad (2a)$$

If we assume a surface with θ of 180^o is also singular, the following equation is established.

$$\gamma(\theta) = \gamma(90^o)\cos\theta + \gamma(180^o)\sin\theta \quad (90^o \le \theta \le 180^o). \qquad (2b)$$

According to a first-principles calculation on diamond and silicon, γ decreases with the increase of hydrogen coverage [24]. Since hydrogen binds more strongly to 4H-SiC (000-1) (i.e., $\theta = 180^o$) than to 4H-SiC (0001) (i.e., $\theta = 0^o$) [25, 26], it is reasonable to assume that $\gamma(180^o)$ is lower than $\gamma(0^o)$. Here we tentatively assume $\gamma(180^o) = 0$ because a surface with $\theta = 180^o$ is hard to appear in trenches formed on (0001) substrates.

Since the growth rate R_g on a surface with $\theta = 90^o$ was reported to be the same as R_g on a surface with $\theta = 0^o$ [22], $\gamma(90^o)$ was reasonably assumed to be equal to $\gamma(0^o)$. In this study, $\gamma(0^o)$ was varied from 0.03 to 0.05 J/m^2, as shown in Fig. 4.

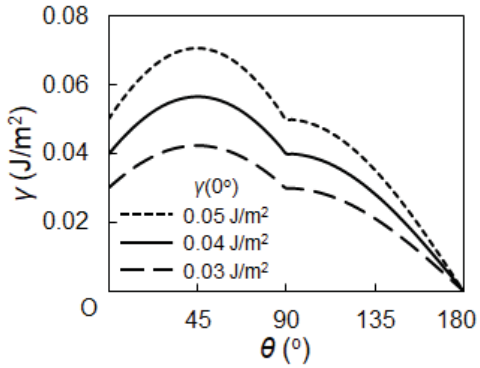

Fig. 4. Assumed γ as a function of θ.

B. Modeling of a SiC-CVD Reactor

A horizontal hot-wall reactor was modeled based on 2D computational fluid dynamics [27]. The chemical reactions considered are listed in Table II. Under the growth conditions listed in Table I, C-to-Si ratio was calculated to be larger than unity at the growth position (Fig. 5), showing vapor-phase diffusion of Si-containing growing species limited the growth of SiC. As stated in Section I, SiCl is most dominant near the

wafer surface among the Si-containing growing species (Fig. 6).

Boundary-layer thickness L_L (Fig. 7) was determined from the minimum height at which the incoming SiCl flux was constant; namely, L_L = 1.5 mm (Fig. 6). The gas-phase concentration of SiCl molecules at the top of the boundary layer (C_{SiCl}^0 = 61.3 μmol/m^3) and the equilibrium gas-phase concentration of SiCl molecules that are in contact with a plane surface [$C_{SiCl}^e(\infty, 1873\ K)$ = 54.3 μmol/m^3] were used as the boundary conditions (Fig. 7) for topography simulation.

TABLE II. CHEMICAL REACTIONS CONSIDERED

1	$C_3H_8 \leftrightarrow CH_3 + C_2H_5$
2	$C_2H_5 + H \leftrightarrow 2\ CH_3$
3	$CH_3 + H_2 \leftrightarrow CH_4 + H$
4	$C_2H_5 \leftrightarrow C_2H_4 + H$
5	$2\ CH_3 \leftrightarrow C_2H_4 + H_2$
6	$C_2H_4 \leftrightarrow C_2H_2 + H_2$
7	$SiH_4 \leftrightarrow SiH_2 + H_2$
8	$SiH_2 \leftrightarrow Si + H_2$
9	$SiH_2 \leftrightarrow SiH + H$
10	$H_2 \leftrightarrow 2\ H$
11	$Si + HCl \leftrightarrow SiCl + H$
12	$SiCl \leftrightarrow Si + Cl$
13	$SiCl + Cl \leftrightarrow SiCl_2$
14	$2\ HCl \leftrightarrow H_2 + 2\ Cl$

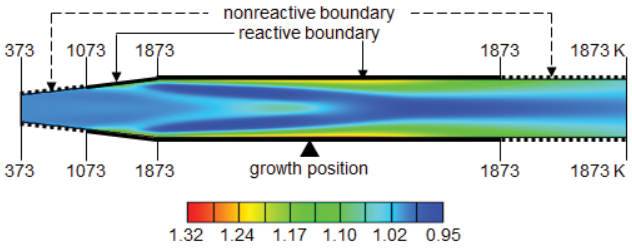

Fig. 5. Calculated C-to-Si ratio and temperature and reactive/nonreactive boundary conditions. Growth conditions are listed in Table I.

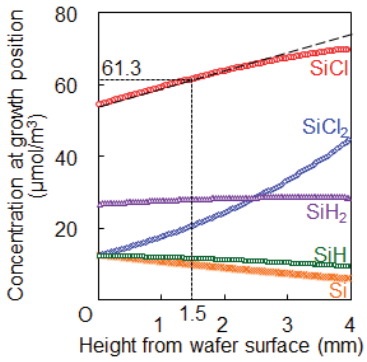

Fig. 6. Concentrations of growing species at growth position as a function of height from wafer surface. Growth conditions are listed in Table I.

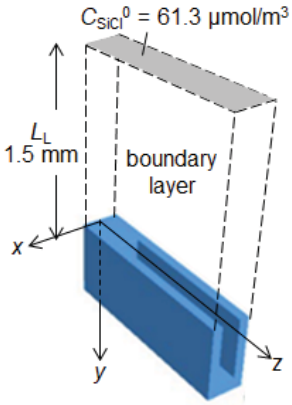

Fig. 7. Schematic illustration of the boundary layer determined by computational fluid dynamics.

C. *Modeling of a Growing Surface*

The surface-reaction rates for SiC CVD based on SiH_4 and C_3H_8 are so fast [28] that R_g in trenches can be determined by the SiCl-diffusion flux as

$$\partial f/\partial t + R_g(\partial f/\partial x + \partial f/\partial y + \partial f/\partial z) = 0 \text{ and} \quad (3)$$

$$R_g = [-D_{SiCl}^{eff}\partial(C_{SiCl}\,|_{\text{growing surface}} - C_{SiCl}^e(r))/\partial \boldsymbol{n}]/V_m, \quad (4)$$

where $f(x, y, z)$ is a level-set function defined as a function of the signed distance from the point (x, y, z) to the growing surface, D_{SiCl}^{eff} is effective SiCl diffusivity determined from the measured growth rate on a simultaneously grown bare wafer (i.e., 0.020 μm/min), and $\boldsymbol{n}$ is the vector normal to the growing surface. Eqs. (1)−(4) were solved using technology computer-aided-design (TCAD) (Victory Process [29]) that use the high-order nonoscillatory schemes for Hamilton-Jacobi equations [30].

III. Topography Simulation

Figure 8 compares the simulated longitudinal (B-B' in Fig. 1) and cross (A-A' in Fig. 1) sections of 3-h grown 4H-SiC trenches with the experimentally observed ones [3, 7]. In the case $\gamma(0^o)$ = 0.03 J/m^2 (doted curve in Fig. 4), a void defect appears in the cross section, which does not agree with the experimental observation. In the case $\gamma(0^o)$ = 0.05 J/m^2 (dashed curve in Fig. 4), no void defects appear in the cross section; however, a dip experimentally observed in the longitudinal section is not reproduced.

In contrast, both an experimentally observed dip in the longitudinal section and a void-free cross section are qualitatively reproduced when $\gamma(0^o)$ is 0.04 J/m^2 (solid curve in Fig. 4).

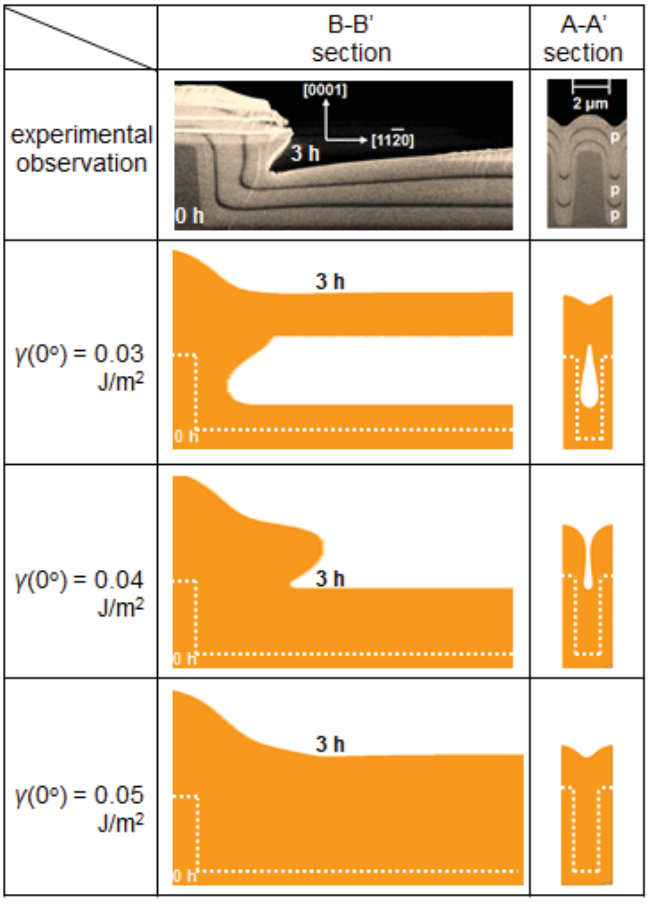

Fig. 8. Experimentally observed [3, 7] and numerically simulated longitudinal (B-B' in Fig. 1) and cross (A-A' in Fig. 1) sections of 4H-SiC trenches grown for 3 h under the conditions listed in Table I.

IV. Discussion

While the longitudinal (B-B' in Fig. 1) section was qualitatively reproduced with $\gamma(0^o)$ of 0.04 J/m^2, the cross (A-A' in Fig. 1) section was better reproduced with $\gamma(0^o)$ of 0.05 J/m^2 (Fig. 8). Such difference in $\gamma(0^o)$ suggests that inclusion of $\gamma(\theta, \varphi)$ should further improve a three-dimensional reproduction of the experimentally observed topography of filled 4H-SiC trenches.

V. Summary

By including a θ dependence of γ in a TCAD topography simulator, both longitudinal and cross sections of 4H-SiC stripe trenches filled by subatmospheric CVD were qualitatively reproduced. Development time for 4H-SiC SJ power devices is to be reduced by the developed topography simulation combined with subsequent TCAD-based process and device simulation.

Acknowledgment

K. Mochizuki thanks Dr. Kunihiro Sakamoto of AIST for expounding an orientation dependence of surface free energy of 4H-SiC.

References

[1] R. Kosugi, et al., "Development of SiC super-junction (SJ) device by deep trench-filling epitaxial growth," Mat. Sci. Forum, vol. 740−742, pp. 785−788, January 2013.

[2] S. Shirota and S. Kaneda, "New type of varacter diode consisting of multilayer p-n junctions," J. Appl. Phys., vol. 49, no. 11, pp. 6012−6019, December 1978.

[3] K. Mochizuki, et al., "First topography simulation of SiC-chemical-vapor-deposition trench filling, demonstrating the essential impact of the Gibbs−Thomson effect," IEDM Tech. Dig., pp. 788−791, December 2017.

[4] R. Kosugi, et al., "First experimental demonstration of SiC super-junction (SJ) structure by multi-epitaxial growth method," Proc. ISPSD, pp. 346−349, June 2014.

[5] Z. Zhong, et al., "Design and experimental demonstration of 1.35 kV SiC super junction Schottky diode," Proc. ISPSD, pp. 231−234, June 2016.

[6] T. Masuda, et al., "0.97 mΩcm^2/820 V 4H-SiC super junction V-groove trench MOSFET," Mat. Sci. Forum, vol. 897, pp. 483−488, May 2017.

[7] S. Ji, et al., "An empirical growth window concerning the input ratio of HCl/SiH$_4$ gases in filling 4H-SiC trench by CVD," Appl. Phys. Express, vol. 10, pp. 055505-1−055505-4, May 2017.

[8] J. P. McVittie, et al., "LPCVD profile simulation using a re-emission model," IEDM Tech. Dig., pp. 917−920, December 1990.

[9] S. M. Gates, "Surface chemistry in the chemical vapor deposition of electronic materials," Chem. Rev., vol. 96, no. 4, pp. 1519−1532, June 1996.

[10] L. Jaouen, et al., "Multiscale modeling of low-pressure CVD of silicon based materials in deep submicronic trenches: a continuum feature scale model," Proc. EUROCVD-15, pp. 111−119 , September 2005.

[11] S. Kinoshita, et al., "Multiscale analysis of silicon low-pressure chemical vapor deposition," Jpn. J. Appl. Phys., vol. 44, no. 11, pp. 7855−7862, November 2005.

[12] S. Yamauchi, et al., "Fabrication of high aspect ratio doping region by using trench filling of epitaxial Si," Proc. ISPSD, pp. 363−366, June 2001.

[13] J. Sakakibara, et al., "600 V-class super junction MOSFET with high aspect ratio p/n columns structure," Proc. ISPSD, pp. 299−302, May 2008.

[14] S. Y. Ji. et al., "Filling 4H-SiC trench towards selective epitaxial growth by adding HCl to CVD process," Appl. Phys. Express, vol. 8, pp. 065502-1−065502-4, June 2015.

[15] K. Hara, et al., "150 mm silicon carbide selective embedded epitaxial growth technology by CVD," Mat. Sci. Forum, vol. 897, pp. 43−46, May 2017.

[16] R. Kosugi, et al., "Strong impact of slight trench direction misalignment from [11-20] on deep trench filling epitaxy for SiC super-junction devices," Jpn. J. Appl. Phys., vol. 56, pp. 04CR05-1−04CR05-4 , April 2017.

[17] http://www.kagaku.com/malt/product.html

[18] C. H. J. van den Brekel and A. K. Jansen, “Interface morphology in chemical vapor deposition on profiled substrates,” J. Cryst. Growth, vol. 43, no. 4, pp. 488−496 , May 1978.

[19] H. J. Oh, et al., “Simulation of CVD process by boundary integral technique,” J. Electrochem. Soc., vol. 139, no. 6, pp. 1714−1720 , June 1992.

[20] H. Liao and T. S. Cale, “Low-Knudsen-number transport and deposition,” J. Vac. Sci. Technol. A, vol. 12, no. 4, p. p1020−1026, July/August 1994.

[21] M. Ren, et al., “Influence of the filling holes on the high temperature characteristics of deep trench superjunction MOSFET,” Proc. IPFA, pp. 1−3 , July 2017.

[22] N. Nordell, S. Karlsson, and A. O. Konstantinov, “Equilibrium crystal shapes for 6H and 4H SiC grown on non-planar substrates,” Mat. Sci. Eng. B, vol. 61−62, pp. 130−134, July 1999.

[23] A. A. Chernov, Modern Crystallography III. Springer-Verlag, Berlin, 1984, p. 13−17.

[24] S. Hong and M. Y. Chou, “Effect of hydrogen on the surface-energy anisotropy of diamond and silicon,” Phys. Rev. B, vol. 57, no. 11, pp. 6262 , March 1998.

[25] T. Seyller, “Passivation of hexagonal SiC surfaces by hydrogen termination,” J. Phys.: Condensed Matter, vol. 16, no. 17, pp. S1755−S1782, April 2004.

[26] E. Wachowicz and A. Kiejna, “Structure and energetics changes during hydrogenation of 4H-SiC {0001} surfaces: a DFT study,” J. Phys.: Condens. Matter, vol. 24, pp. 385801-1−385801-7, September 2012.

[27] http://str-soft.com/products/Virtual_Reactor/VR_CVD_SiC/index.htm

[28] T. Kimoto, et al., “Growth mechanism of 6H-SiC in step-controlled epitaxy,” J. Appl. Phys., vol. 73, no. 2, pp. 726−732 , January 1997.

[29] https://www.silvaco.com/products/tcad/process_simulation/victory_process/victory_process

[30] S. Osher and C.-W. Shu, “High order essentially nonoscillatory schemes for Hamilton-Jacobi equations,” SIAMJ. Numer. Anal., vol. 28, no. 4, pp. 907−922, July 1991.